ACS OMEGA

Open Access

http://pubs.acs.org/journal/acsodf

Article

Novel Bioproduction of 1,6-Hexamethylenediamine from L-Lysine Based on an Artificial One-Carbon Elongation Cycle

Kaixing Xiao, Dan Wang,* Xuemei Liu, Yaqi Kang, Ruoshi Luo, Lin Hu, and Zhiyao Peng

Cite This: *ACS Omega* 2024, 9, 40970−40979

Read Online

ACCESS | Metrics & More | Article Recommendations | Supporting Information

ABSTRACT: 1,6-hexamethylenediamine (HMD) is an important precursor for nylon-66 material synthesis, while research on the bioproduction of HMD has been relatively scarce in scientific literature. As concerns about climate change, environmental pollution, and the depletion of fossil fuel reserves continue to grow, the significance of producing fundamental chemicals from renewable sources is becoming increasingly prominent. In recent investigations, the bioproduction of HMD from adipic acid has been reported but with lingering challenges concerning costly raw materials and low yields. Here, we have undertaken the reconstruction of the HMD synthetic pathway within *Escherichia coli*, which was constituted with L-lysine α-oxidase (*Raip*), *LeuABCD*, α-ketoacid decarboxylase (*KivD*), and transaminases (*Vfl*), leveraging a carbon chain extension module and a metabolic pathway of transaminase-decarboxylase cascade catalysis within the strain WD20, which successfully produce 46.7 ± 2.0 mg/L HMD. To increase the cascade activity and create a higher tolerance to external environmental disturbance for L-lysine to convert into HMD, another two enzymes D-alanine aminotransferase (Dat) and alpha-ketoacid decarboxylase (KdcA) were introduced into WD21 to provide flux flexibility for α-ketoacid metabolization, which was named "Smart-net metabolic engineering" in our research, and high-efficiency synthesis of HMD utilizing L-lysine as the substrate has been successfully achieved. Finally, we established a + 1C bioconversion multienzyme cascade catalyzing up to 65% conversion of L-lysine to HMD. Notably, our fermentation process yielded an impressive 213.5 ± 8.7 mg/L, representing the highest reported yield to date for the bioproduction of HMD from L-lysine.

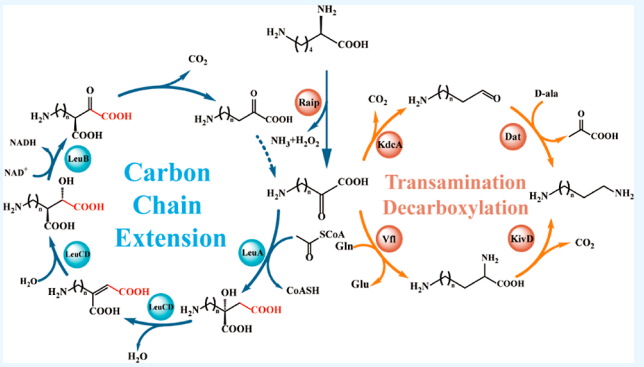

INTRODUCTION

Nylon, academically known as polyamide (PA), is the earliest fiber material first developed by Dupont company, which was industrialized in 1939.[1] In the 1950s, men began to develop and produce injection molded nylon products to replace metals and meet the requirement in lightweight and cost reduction of downstream industrial products.[2] Nylon is a versatile polymer with applications in textiles for clothing, socks, and carpets as well as in engineering for plastics and in the manufacture of ropes, fishing nets, and tire cord fabric. A wide variety of PAs exist, including but not limited to PA6, PA66, PA46, PA610, PA612, and PA1010. In recent years, there has been a surge in the development of new semiaromatic nylons like PA6T, as well as specialized nylons, which are being utilized as advanced engineering plastics.[3] The worldwide market for nylon, valued at approximately USD 28.5 billion in 2019, is projected to achieve a compound annual growth rate of 6.5% in terms of revenue during the forecast time frame. The increasing production and sales volumes in the automotive industry, coupled with advancements in manufacturing, are expected to fuel the demand for nylon.

In recent years, enterprises and academic circles began to pay attention to nylon production from biobased sources. Traditional chemical production of nylon can lead to environmental issues such as pollution, high energy use, and nondegradable waste. Enhancing production methods and using eco-friendly chemicals can reduce pollution in nylon manufacturing, utilizing efficient and renewable energy can lessen its climate impact, recycling and repurposing nylon conserves resources and reduces the need for new inputs, and developing biobased nylon from sustainable resources can decrease dependence on fossil fuels. 6-Aminocaproic acid (6-ACA) is a monomer for nylon-6 and can traditionally be synthesized from caprolactam. But recently, it has been reported that 6-ACA could be produced from glucose or lysine by engineered microbes. Through the condensation of acetyl-CoA and succinyl-CoA, engineered *Escherichia coli* (*E. coli*) could produce 6-ACA at a titer of 160 mg/L[5]. In our lab,

Received: July 7, 2024
Revised: August 30, 2024
Accepted: September 5, 2024
Published: September 17, 2024

an artificial *LeuABCD* operon along with decarboxylase and transaminase, could turn the substrate lysine to 6-ACA with a titer of 24.1 mg/L by engineered strain.[6] Adipic acid (AA) and 1,6-hexamethylenediamine (HMD) are two building blocks for nylon-66. AA could be produced from glucose at a titer of 2.23 g/L by engineered *Thermobifida fusca*, be produced from fatty acids at a titer of 50 g/L by engineered *Candida* spp and be synthesized from glycerol at a titer of 68 g/L by engineered *E. coli*.[7] Several patents propose various non-natural metabolic pathways for HMD biosynthesis, even a paper reported enzyme catalysis for HMD synthesis from AA with a 30% conversion,[4] there are studies that have utilized cyclohexane, cyclohexanol, or AA to produce adiponitrile, and they have achieved quite remarkable results,[8−10] while HMD production from L-lysine by engineered microbes in vivo has not yet been achieved.

L-Lysine ranks second highest in global production among amino acids. It is primarily manufactured via microbial fermentation using sustainable biomass sources. L-Lysine serves various purposes, including its use as a food additive, a dietary supplement, and in the realm of animal nutrition.[11−13] Due to the market crisis in industrial overcapacity and fierce international competition faced by companies in this industry, developing high-value chemicals derived from L-lysine presents an opportunity to construct an integrate supply chain and maintain the price of lysine.[14] To construct the biosynthesis of non-natural metabolic pathway from L-lysine to HMD in vivo, the structural differences between lysine and HMD were examined, which might require a decarboxylation and deamination reaction of lysine and one carbon extension conversion to become HMD. Inspired by the artificial *LeuABCD* cycle[15] which we have engineered to operate for 6-aminocaproate production, it was hypothesized that lysine could be degraded to 2-keto-6-aminocaproate by the action of lysine oxidase (*Raip*), and the specific information about the enzymes can be found in Table S3. Then, one carbon is added by *LeuABCD*-catalyzed carbon chain extension. While the 7C ketoacid is formed, the module of decarboxylation and transamination could be performed for HMD synthesis. This method represents a notable departure from the existing methods for HMD production.

Decarboxylase enzymes, which utilize Mg^{2+} and thiamin diphosphate (ThDP) as cofactor, mainly catalyze the non-oxidative decarboxylation of 2-keto acids,[16] it has been used in the construction of artificial pathways for non-natural alcohol biosynthesis. In previous site-directed mutagenesis experiments on decarboxylase, such as pyruvate decarboxylase, benzoylformate decarboxylase, and indole pyruvate decarboxylase, it was shown that a single mutation can significantly enhance the decarboxylase activity for long-chain (C5/C6) aliphatic keto acids.[17] The enzymatic decarboxylation reaction of 7-amino-2-oxoheptanoic acid was aimed to be catalyzed using alpha-ketoacid decarboxylase (*KivD*) and branched-chain alpha-ketoacid (*KdcA*) decarboxylase from *Lactococcus lactis*. *KivD* has been proved that enable specific production of longer-chain (C5−C8) alcohols from sugar, the specific regulation of *KivD* on 1-pentanol synthesis was achieved by mutagenesis of the V461 residue.[18] KdcA functions as a multifaceted catalyst in the creation of enantioselective 2-hydroxy ketones, notable for its remarkably expansive capacity to accommodate a variety of substrates.[19] In reactions catalyzed by KdcA, the roles of acceptor and donor are assigned based on the specific substrates selected. 2-Oxo acids predominantly act as donor substrates, whereas the corresponding aliphatic aldehydes are typically the chosen acceptor substrates. This preference is attributed to the compulsory decarboxylation process that 2-oxo acids undergo before the carboligation step.[20] Therefore, fixing of the acceptor versus donor role is also preferred to catalyze the reaction from 7A2OPA to 6-aminoexanal. Aminotransferase is well characterized as pyridoxal 5′-phosphate (PLP)-dependent enzyme that catalyzes reversible transfer of an amino group between amino acid and keto acid.[21−23] The catalytic mechanism and structural topology of aminotransferases,[24] especially aromatic amino acid aminotransferase (AroAT) and L-aspartate aminotransferase (AspAT), have been deeply studied, and their substrate recognition mechanisms have been successfully explained.[25,26] Due to the broad substrate specificity of the aminotransferase, various amino donors and amino acceptors were used to explore the active site structure in Shin's research.[27] In this study, amino groups are expected to be transferred to 6-aminohexanal by special aminotransferase, with alanine or glutamine as the amine donor.

The natural metabolic mechanism of organisms is complex, which is not fully understood by humans yet. However, great efforts are made in this field, and some principles are revealed and accepted by academia people.[28] Adaptation to the environment is essential for organism survival. Typically, glycolysis occurs in environments lacking oxygen. However, under conditions of fasting or starvation, the activation of forkhead transcription factors FOXK1 and FOXK2 promotes aerobic glycolysis. This is achieved by increasing the expression of enzymes necessary for glycolysis and concurrently inhibiting the oxidation of pyruvate in the mitochondria through the upregulation of pyruvate dehydrogenase kinases.[29] Following the principles of recycling and metabolic adaptability, microorganisms within the plutonic crust can endure fissures or porous materials. They do so by linking available energy sources to both organic and inorganic carbon supplies, which are likely supplied via the movement of fluids beneath the seabed or by seawater infiltration.[30] *Galdieria sulphuraria* is reported with an enormous metabolic flexibility, and it lives in hot, toxic metal-rich, acidic environments, growing either photo autotrophically or heterotrophically on more than 50 carbons.[31] When constructing an engineered strain for the purpose of HMD production, we aimed to emulate natural processes and developed a strategy termed "Smart-net metabolic engineering", designed to leverage the strain's metabolic flexibility and enhance its robustness.

In this study, the capability of *LeuA*BCD* to facilitate the one-carbon conversion of lysine-derived 2K6AC was demonstrated. The HMD production was subsequently achieved with decarboxylase and transaminase catalysis. A prokaryotic variant of decarboxylase, exhibiting enhanced expression in *E. coli*, was identified and performed well in the cascade catalysis with substrate preference for 7C amino acid. Using this variant, this artificial system for +1C elongation and HMD production was implemented. To increase the HMD titer, another two enzymes D-alanine aminotransferase (*Dat*) and alpha-ketoacid decarboxylase (*KdcA*) were introduced into WD21 to provide flux flexibility for α-ketoacid metabolization, which was transaminated first before be decarboxylated. We endeavor to emulate natural processes, thereby endowing engineered microbes with the robustness necessary to adapt to significant fluctuations in external environmental conditions.

https://doi.org/10.1021/acsomega.4c06289
ACS Omega 2024, 9, 40970−40979

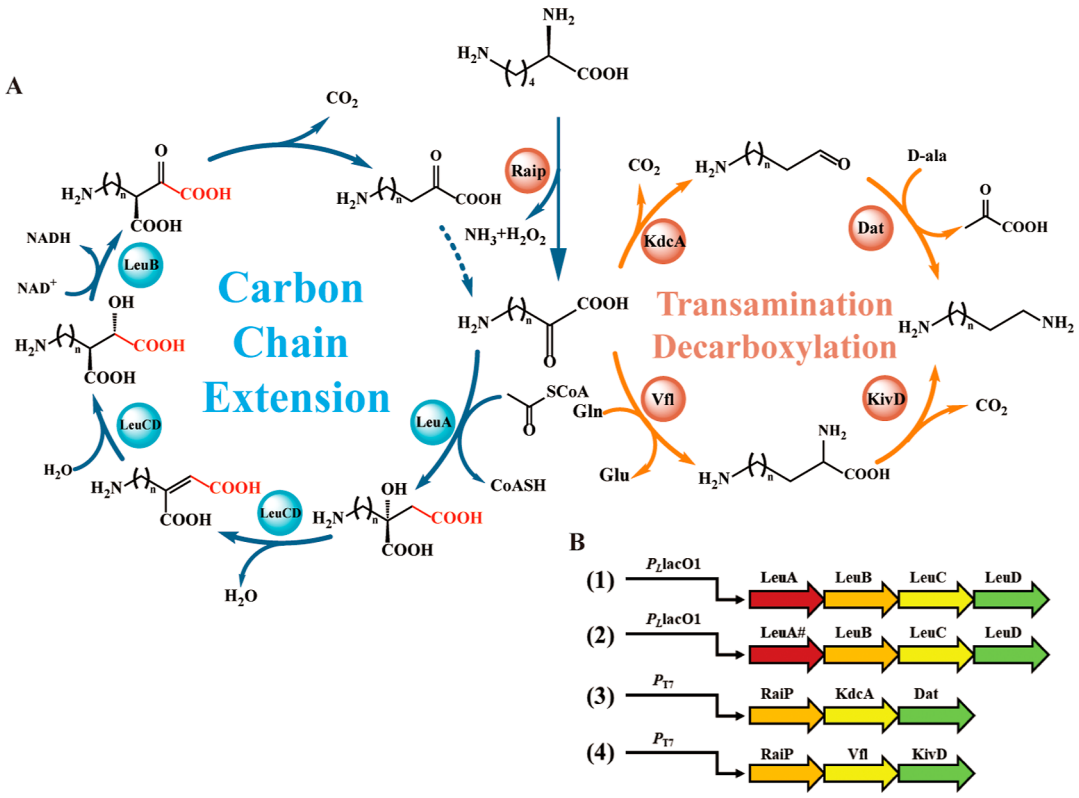

Figure 1. (A) Engineered artificial iterative carbon-chain-extension cycle to produce HMD. (B) Synthetic operons for gene expression. (1) Synthetic operon for protein overexpression to drive the carbon flux toward 2K6AC. (2) Synthetic operon carrying mutations of *LeuA* (*LeuA*$^{\#}$) for protein overexpression to drive the carbon flux toward 2K6AC. (3) Synthetic operon for protein overexpression for decarboxylase and transaminase. *Raip*, L-lysine α oxidase; *LeuA*, α-isopropylmalate synthase; *LeuA**, *LeuA* mutants; *LeuA*$^{\#}$, *LeuA* with H97L/S139G/G462D mutations; *LeuB*, 3-isopropylmalate dehydrogenase; *LeuC*, 3-isopropylmalate dehydratase; *LeuD*, 3-isopropylmalate dehydratase; *KdcA*, alpha-ketoacid decarboxylase; *Dat*, D-amino acid transaminase; *Vfl*, pyruvate transaminase; and *KivD*, α-ketoacid decarboxylase.

RESULTS AND DISCUSSION

Thermodynamic Analysis of the Proposed HMD Synthesis Cycle. Our preceding studies have established *LeuABCD* as a viable metabolic entry point. In this investigation, a duo of theoretical HMD biosynthetic routes, initiating from the extension of the L-lysine carbon skeleton, has been conceptualized, proceeding via (i) decarboxylation complemented by transamination, or (ii) transamination succeeded by decarboxylation, as illustrated in Figure 1. To appraise the feasibility of the transamination and decarboxylation cascade, the standard Gibbs free energy change for these reactions was computationally predicted under physiologically relevant conditions, enumerated in Table S1. This analysis is imperative for elucidating the thermodynamic favorability inherent in the proposed enzymatic routes.

According to the relevant calculations, the Gibbs free energy of path i is -157.39 kJ·mol^{-1}, and that of path ii is -144.64 kJ·mol^{-1}. The detailed information is shown in Table S1. It seems that path i is more thermodynamically feasible than path ii. If the 7C compound α-ketoaminoheptanic acid is formed, decarboxylation reaction might first occur, be preferred more than the transamination reaction. In summary, these calculations suggested that our designed synthetic pathways might provide promising solutions to the production of HMD, which might compete with nowadays oil-refining methods[11] or AA-based enzymatic methods as reported.[4]

HMD Was Synthesized through a Multienzymatic Cascade that Integrated Carbon Chain Elongation and Transamination-Decarboxylation Strategies. In this study, two different engineered catalytic pathways were constructed to produce HMD, as indicated by the theoretical calculations in the last section. To explore the feasibility of the *Raip-LeuA*$^{\#}$*BCD-KdcA-Dat* pathway in vitro, the necessary enzymes were expressed, purified, and detected. The recombinant proteins *Raip*, *LeuA**, *LeuB*, *LeuC*, *LeuD*, *KdcA*, and *Dat* carrying C-terminal His-tag in *E. coli* BL21(DE3) was detected by SDS-PAGE shown in Figure S1. Respectively, the sizes of recombinant proteins were 55, 52, 38, 50, 21, 62, and 31 kDa, which were consistent with the predicted size of *Raip*, *LeuA*, *LeuB*, *LeuC*, *LeuD*, *KdcA*, and *Dat*. Similarly, the *Raip-LeuA*BCD-Vfl-KivD* pathway in vitro was also constructed, and individual proteins were overexpressed, purified, and detected by SDS-PAGE, also shown in Figure S1.

LeuA had a low activity to 2K6AC, as has been presented in our recent research,[6] LeuA H97L/S139G/G462D (*LeuA*$^{\#}$) was used as the enzyme to initiate the carbon chain elongation cycle. *LeuA*$^{\#}$ showed a great activity of 0.03 unites/mg toward 2K6AC, which is the lysine derivative produced by the *Raip* enzyme. Based on the success of the individual protein's expression and purification, the "+1" carbon chain extension pathway was combined with subsequent α-keto acid decarboxylation and transamination to produce diamines. As estimated, *Raip-LeuA*$^{\#}$*BCD* was the successful artificial pathway to iterate the carbon extension in biosynthesis using a cyclic pathway. After the addition of one carbon by this pathway, 7-amino-2-oxoheptanoic acid, a substrate derived from L-lysine, can exit the circulation pathway through *KdcA* and *Dat* to

https://doi.org/10.1021/acsomega.4c06289
ACS Omega 2024, 9, 40970−40979

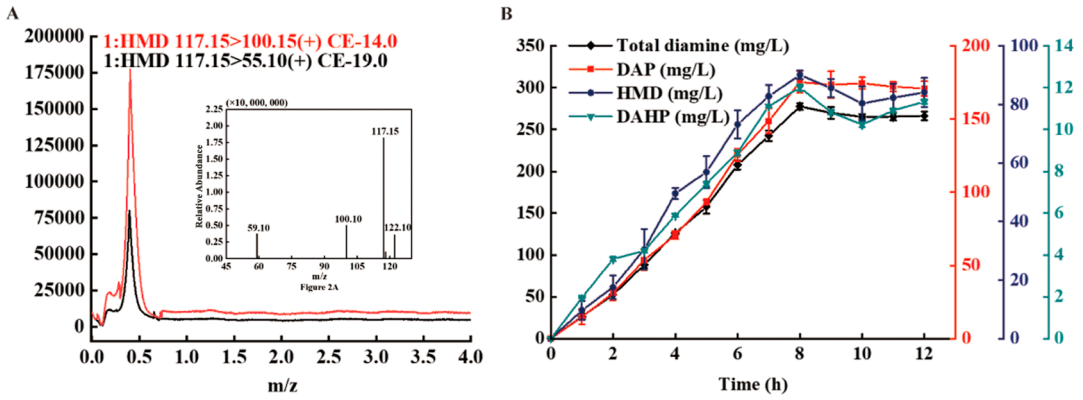

Figure 2. (A) LC−MS confirmation of NNSCAAs (DAP, HMD, and DAHP) biosynthesis by strain WD21. (B) HPLC results of DAP, HMD, and DAHP from fermentation broth. Samples were derived with phenyl isothiocyanate for LC−MS analysis. Strain WD21 is the strain BL21(DE3) harboring plasmids pIVC2 and pET21aRKD. DAP, 1,5-diaminopentane; HMD, 1,6-hexamethylenediamine; and DAHP, 1,7-diaminoheptane.

produce the destined chemical HMD. Due to the promiscuity of *KdcA* and *Dat*, a series of diamines, including pentanediamine, were found among the products, HMD and heptadiamine, as shown in Figure 2. The titer of total diamine was 126.3 ± 5.5 mg/L after a reaction time of 4 h with enzyme concentrations of *Raip*, *LeuA*, *LeuB*, *LeuC*, *LeuD*, *KdcA*, and *Dat* setting at 1.0, 20.0, 4.0, 3.0, 5.0, 5.0, and 2.0 μM, respectively, in a total volume of 250 μL reaction buffer. The distribution of pentanediamine, HMD, and heptadiamine was 12.0:8.4:1. As shown in Figure 2, the titer of total diamines reached 277.5 ± 9.4 mg/L after reaction for 8 h in a total volume of 250 μL of reaction buffer, and the distribution of pentanediamine, HMD, and heptadiamine was 14.6:7.5:1. The products' identities were confirmed through liquid chromatography−mass spectrometry (LC−MS) analysis, as shown in Figure 2.

Drawing on the enzyme catalytic characteristics determined through in vitro assays, we endeavored to design an artificial iterative metabolic route. An engineered *E. coli* strain producing HMD was obtained by expressing seven enzymes (*Raip*, *LeuA*$^{\#}$, *LeuB*, *LeuC*, *LeuD*, *KdcA*, and *Dat*). As shown in Figure 3, the resulting engineered *E. coli* strain produces total diamines at a titer of 1.66 g/L from L-lysine in a 250 mL shake flask filled with 50 mL of fermentation medium. After 36 h of aerobic cultivation, there was no accumulation of HMD in the control strain, whereas the engineered strain produced HMD with a peak concentration of 36.3 ± 2.4 mg/L at 36 h. The successful integration of this repetitive pathway in *E. coli* confirms the efficacy of the in vitro designed pathway for synthesizing diamines derived from L-lysine.

As of now, the L-lysine-derived pathway described herein stands at the forefront of metabolic engineering, being the inaugural instance to harness iterative carbon extension in conjunction with decarboxylation and transamination for the biosynthetic generation of 1,6-hexanediamine (HMD) within a living cellular factory. The enigmatic cyclicality inherent to the carbon extension pathway not only enables the concomitant biosynthesis of pentanediamine, HMD, and heptadiamine but also underscores an exceptional metabolic adaptability. This plasticity is a testament to the pathway's potential for further refinement, whether it be in the diversification of substrate metabolism or in the fine-tuning of product yield and specificity. Recognizing the pivotal role that pentanediamine, HMD, and heptadiamine play as precursors in the polymerization cascade leading to PAs, there exists a burgeoning body

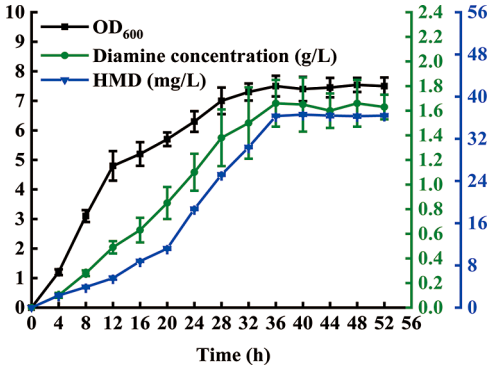

Figure 3. NNSCAA synthesis by engineered strain WD21 in a 250 mL flask. The cells were grown in 50 mL of LB supplemented with 100 μg/mL ampicillin, 50 μg/mL kanamycin, 0.5 mM of IPTG, 5 g/L L-lysine, 1.0 mM $MgSO_4$, and 0.5 mM ThDP at 37 °C with 250 rpm orbital shaking. Strain WD21 is strain BL21(DE3) plus plasmids pIVC2 and pET21aRKD. The total diamines conclude DAP, HMD, and DAHP. DAP, 1,5-diaminopentane; HMD, 1,6-hexamethylenediamine; and DAHP, 1,7-diaminoheptane. Each experiment was conducted at least three times to ensure reliability and data are presented as mean values ± SD.

of scientific inquiry dedicated to the optimization of their microbial production. This research thrust is driven by the overarching goal of enhancing the efficiency, selectivity, and sustainability of bioprocesses for the generation of these high-value, industrially relevant platform chemicals.[5] The pentanediamine was the most extensively researched, while *LdcEt* was used for the directly decarboxylation of lysine to produce about 165.96 g/L of pentanediamine, which has a potential to be industrialized.[32] The HMD was reported to be produced through enzyme catalysis from AA only,[4] while AA is now an oil-refining product. A novel biosynthetic strategy for the concurrent production of C5, C6, and C7 diamines from chain-elongated biolysine was developed, focusing on enhancing yield and selectivity through engineered microbial pathways. For this, the promiscuity of LeuA mutants toward L-lysine-derived α-ketoacids was adopted in our lab, and the experimental data confirmed that LeuA$^{\#}$ is capable of using primary amines, including compounds like 2K6AC and 2-keto-7-aminoheptanoate, as substrates. Also, the functional ability of *KdcA*, *Dat*, *Vfl*, and *KivD* was explored for the cascade decarboxylation and transamination, and their substrate profiles remained to be further explored. Because of the

https://doi.org/10.1021/acsomega.4c06289
ACS Omega 2024, 9, 40970−40979

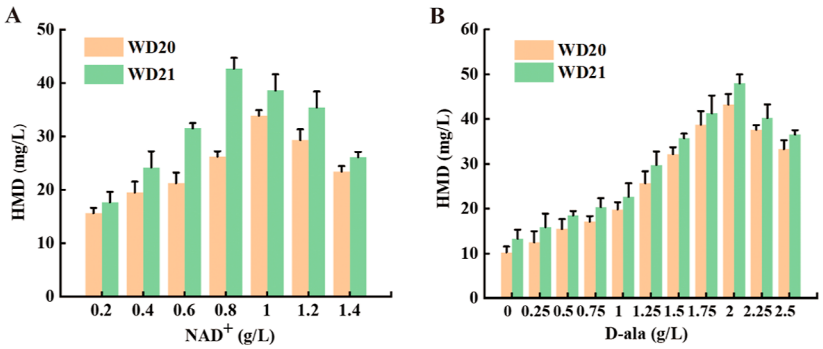

Figure 4. (A) Synthesis of NNSCAAs from L-lysine was carried out using a variety of NAD^+ concentrations. (B) Manufacturing process of NNSCAAs from L-lysine involved conducting reactions with varying levels of D-alanine. Each assay mixture included 2.0 mM acetyl-CoA, 1.0 μM *Raip*, 20.0 μM *LeuA*$^{\#}$, 4.0 μM *LeuB*, 2.0 μM *LeuC*, 2.0 μM *LeuD*, 5.0 μM *KdcA*, 2.0 μM *Dat*, 5.0 μM *KivD*, 2.0 μM *Vfl*, 2.5 mM L-lysine, 1.0 mM $MgCl_2$, 1.0 mM TCEP, and 0.5 mM ThDP. Reactions incubated for 8 h at 37 °C. Each experiment was conducted at least three times to ensure reliability and data are presented as mean values ± SD.

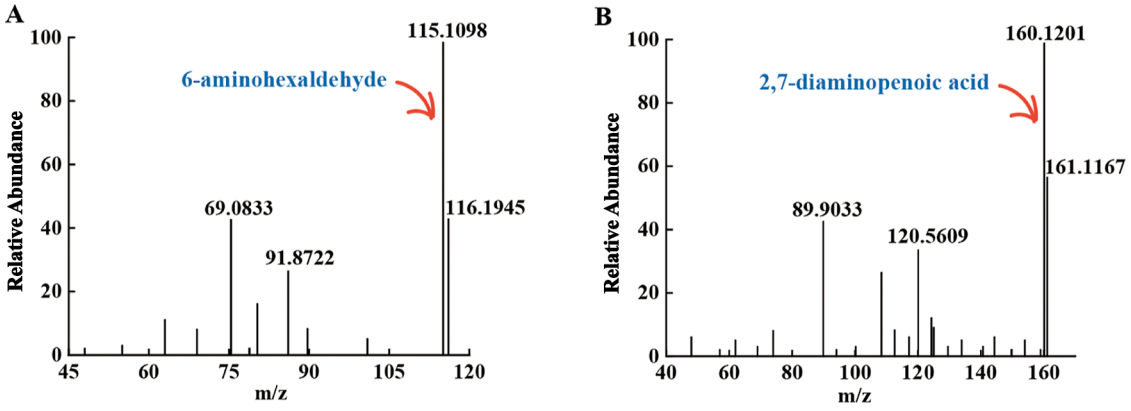

Figure 5. LC−MS confirmation of 6-aminohexanal and 2,7-diaminoheptanoic acid biosynthesis by strains. (A) Mass spectrum results of 6-aminohexanal from fermentation broth by strain WD21. Strain WD21 is strain BL21(DE3) plus plasmids pIVC2 and pET21aRKD. (B) Mass spectrum results of 2,7-diaminoheptanoic acid from fermentation broth by strain WD20. Strain WD20 is strain BL21(DE3) plus plasmids pIVC2 and pET21aRVK.

rapid propagation of microorganisms, our biosynthesis method is better than the enzymatic synthesis previously reported. Our substrate is lysine, which means that we can completely get rid of our dependence on oil resources and establish a new biobased HMD production line. In the future, the gene of the lysine production pathway can also be transferred into engineered strains to construct an integrated biosynthetic pathway for HMD production from bulk feedstock glucose.

Optimization of the HMD Biosynthetic Pathway by a Multienzymatic Complex System. NAD^+ is a key coenzyme of LeuB in this artificial iterative cycle pathway. *KdcA* and Dat catalyze the conversion of 2-keto-7-amino-heptanoic acid into HMD, as same as *Vfl* and *KivD*, both require the coenzyme NAD^+. To increase the yield of HMD, the concentration of NAD^+ was optimized. The results showed that HMD was produced by NAD^+ with varying concentrations at pH 8.0 for 8 h within 50 mL of fermentation medium. As shown in Figure 4, the concentration of NAD^+ affects the production of HMD. The multienzyme cascade system necessitates the supplementation of NAD^+ for the generation of HMD. Upon the introduction of 0.2 g/L NAD^+, the concentration of HMD achieved was 17.6 ± 0.8 mg/L. With the increase of NAD^+ concentration, the titer of HMD production was also increased. When NAD^+ concentration was 0.8 g/L, the HMD concentration was 42.7 ± 4.2 mg/L. Therefore, 0.8 g/L NAD^+ was the best dosage. Due to the conversion of D-ala into pyruvate during the process of ammonia conversion, the fermentation conditions were optimized with different concentrations of D-ala addition. The multienzyme cascade system produced only 13.29 ± 0.7 mg/L HMD without the addition of D-ala. When 1.0 g/L D-ala was added, the titer of HMD was 22.64 ± 1.5 mg/L. The concentration of HMD increased to 47.96 ± 2.1 mg/L when the D-ala supplemental level was 2.0 g/L. As the dosage of D-ala continuously increased, the titer of HMD decreased, and 2.0 g/L D-ala was the optimal concentration. Taking it a step further, to scale up HMD production, effective separation and purification from fermentation broth are crucial for quality and commercial viability. Designing scalable separation processes that balance operational costs, recovery rates, and purity is critical. Technological innovations, including membrane separation engineering, integrated systems, and AI optimization, enhance efficiency and reduce costs, driving HMD toward industrial application.

Confirmation of the Intermediates Indicating the Enzyme Cascades Sequence. In this study, the biotransformation from L-lysine to HMD was conducted using RaipKD; then, RaipVK was also used as the second line to produce HMD. However, the mechanism behind it is not yet clear. In this study, LC−MS and NMR were performed to prove the existence of intermediate products and to deduce the sequence of the enzymatic reactions.

https://doi.org/10.1021/acsomega.4c06289
ACS Omega 2024, 9, 40970−40979

LC−MS was used to analyze the intermediate and final products of biotransformation catalyzed by *Vfl* and *KivD*. As shown in Figure 5, 2,7-diaminopenoic acid was found in the fermentation broth. 2,7-diaminoheptanoic acid was the product of 2-keto-7-aminoheptanoic acid via transamination of *Vfl* and then to produce HMD by decarboxylation of *KivD*. It was confirmed that the synthesis of HMD from 2-keto-7-amino heptanoic acid using *Vfl* and *KivD* was a process of transamination followed by decarboxylation. Whereas 2,7-diaminoheptanoic acid was an unnatural compound, it has not been described in the natural environment. Similarly, a LC−MS analysis showed that the intermediate 6-aminohexaldehyde existed in the fermentation broth of RaipKD, as shown in Figure 5. It was also confirmed that using *KdcA* and *Dat* was a sequential process, which was decarboxylation followed by transamination.

Smart-Net Metabolic Engineering for HMD Synthesis. All four transamination and decarboxylation enzymes were expressed in the cell simultaneously, and as it could be seen from Figure 6, when Gln and D-ala was fed individually, the

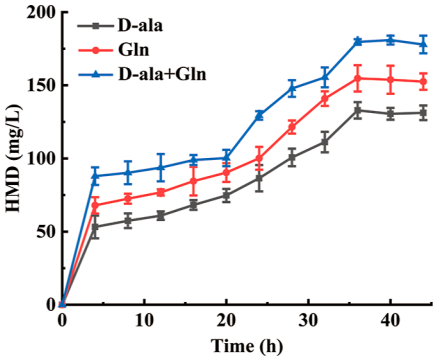

Figure 6. Effect of different amine donors on HMD yield. The yield of HMD was measured individually when Gln was added alone, D-ala was added alone, and Gln and D-ala were both added. All experiments were performed a minimum of three independent sets. Each experiment was conducted at least three times to ensure reliability, and data are presented as mean values ± SD.

strain could respectively produce HMD in a titer of 154.7 ± 10.1 and 132.9 ± 9.9 mg/L within 50 mL of fermentation medium. While Gln and D-ala was fed simultaneously, the pathway the strain adopted is depending on the energy state of the cell. When the adenosine 5′-triphosphate (ATP) level of the strain is relatively lower at 3.9×10^{-4} to 2.17×10^{-3} nmol/mL as detected, the intermediate product 6-aminohexanal would be higher. This means that when the energy of host was insufficient, the metabolic path the strain chose by itself was decarboxylation first, followed by transamination. The D-ala supplemented was converted into pyruvate to go through the tricarboxylic acid cycle to provide a higher amount of ATP for the host. If the cell has been fed with a higher level of Gln and the cell is in a high ATP state by electric or other means, the production of intermediate 2,7-diaminoheptanoic acid is going to be higher, which means that *Vfl* has been activated to transform of Gln to Glu first, which also stored energy for the host strain. The phenomenon proved that the metabolic network has flexibility, choosing different routes to synthesize HMD under different conditions. This "smart-net metabolic engineering" constructed in our research leads to an increased titer of HMD in the different energetic state of the living cell.

The cellular metabolic machinery, with glucose and pyruvate as quintessential substrates, is critical for energy metabolism and carbon assimilation, which is fundamental for cellular proliferation. Pyruvate's metabolic fate as acetyl-CoA is the gateway to the mitochondrial citric acid cycle and oxidative phosphorylation, yielding a substantial ATP endowment for cellular processes. The glycolytic conversion of glucose to pyruvate is a testament to metabolic frugality and efficiency, netting an ATP profit that exemplifies the pathway's adept energy transduction. Metabolic partitioning of resources is dynamically adjusted based on the cellular metabolic status, with the cell's enzymatic repertoire dictating the synthesis of desired products in response to environmental stimuli. This intricate metabolic regulation ensures that the biosynthetic output is tailored to both cellular objectives and extracellular conditions.

CONCLUSIONS

In this study, we engineered a pioneering biosynthetic strategy to produce a HMD in *E. coli*, harnessing dual metabolic pathways. This approach paves the way for a sustainable and industrially viable process for converting renewable feedstocks into a HMD via metabolic engineering. We achieved an in vitro HMD yield of 213.5 ± 5.8 mg/L by integrating a smart-net metabolic engineering strategy with meticulous condition optimization. Identifying rate-limiting enzymes within this engineered iterative reaction sequence, we anticipate enhancements through the application of directed evolution techniques. The successful biosynthesis of HMD through an artificial iterative carbon chain extension cycle illustrates the potential of this strategy to be adapted to produce other amino acids with varying chain lengths and functional groups, such as $-NH_2$ and $-SO_3H$.

MATERIALS AND METHODS

Strains and Culture Conditions. All strains used in this study are given in Table 1. *E. coli* DH5α was employed for gene cloning and plasmid propagation, and *E. coli* BL21 (DE3) and its derivatives were used for HMD production. LB medium (10 g/L tryptone, 10 g/L NaCl, and 5 g/L yeast extract) was used for culturing *E. coli* cells for plasmid construction with proper antibiotics supplemented as follows: 100 μg/mL of ampicillin and 50 μg/mL of kanamycin. *E. coli* strains containing the respective plasmids were inoculated from glycerol reserves and spread onto LB agar plates supplemented with suitable antibiotics. These plates were incubated at a temperature of 37 °C for an extended period, typically overnight.

Construction of Plasmids. All primers used in this study are listed in Table S2. The coding regions of *LeuA*, *LeuB*, *LeuC*, and *LeuD* were amplified from *E. coli* MG1655 by polymerase chain reaction (PCR) using appropriate primers as mentioned by Cheng et al.[6] The PCR product and pET21a+ plasmid were digested by NdeI and XhoI and then ligated into pET21a+ using the T4 DNA ligase to form the engineered pET21a-*leuA-leuB-leuC-leuD*, also named as pWD01. *LeuA* was replaced by $LeuA^{\#}$ (*LeuA**, *LeuA* with H97L/S139G mutations) to form the engineered pET21a-$leuA^{\#}$-*leuB-leuC-leuD*, also named as pWD02.

The nucleotide sequences of genes *Raip* from *Scomber japonicas* (*S. japonicas*), *kivD* from *L. lactis*, and *Dat* from *Bacillus subtilis*, *kdcA* from *L. lactis*, and *vfl* from *Vibrio fluvialis*

https://doi.org/10.1021/acsomega.4c06289
ACS Omega 2024, 9, 40970−40979

Table 1. List of Strains and Plasmids Used in This Study

strains and plasmids	relevant genotype or description	source
	strains	
DH5α	wild type	Novagen
BL21(DE3)	wild type	Sangon
WD20	BL21(DE3) harboring pWD01 and pETaRVK	this study
WD21	BL21(DE3) harboring pWD02 and pETaRKD	this study
	Plasmids	
pET21a	empty plasmid used as control, Amp^R	Sangon
pZA22	empty plasmid used as control, Kan^R	Sangon
pWD01	pET21a-*raip*, pET21a carries a l-lysine α-oxidase (*Raip*) gene from *Scomber japonicas* with *Nde*I and *BamH*I restrictions, Amp^R	this study
pETaRaip	pET21a-*raip*, pET21a carries a l-lysine α-oxidase (*Raip*) gene from *Scomber japonicas* with *Nde*I and *Xho*I restrictions, Amp^R	this lab
pETaleuA	pET21a-*leuA*, pET21a carries a 2-isopropylmalate synthase (*leuA*) gene from *Escherichia coli*, Amp^R	this lab
pETaleuA*	pET21a-*leuA**, pET21a carries a 2-isopropylmalate synthase mutant (H97L/S139G/G462D) gene from *Escherichia coli*, Amp^R	this lab
pETaleuB	pET21a-*leuB*, pET21a carries a 3-isopropylmalate dehydrogenase (*leuB*) gene from *Escherichia coli*, Amp^R	this lab
pETaleuC	pET21a-*leuC*, pET21a carries a 3-isopropylmalate dehydratase large subunit (*leuC*) gene from *Escherichia coli*, Amp^R	this lab
pETaleuD	pET21a-*leuD*, pET21a carries a 3-isopropylmalate dehydratase small subunit (*leuD*) gene from *Escherichia coli*, Amp^R	this lab
pETaKivD	pET21a-*KivD*, pET21a carries an α-ketoacid decarboxylase (*kivD*) gene from *Lactococcus lactis*, Amp^R	this lab
pETaKdcA	pET21a-*KdcA*, pET21a carries an alpha-ketoacid decarboxylase (*KdcA*) gene from *Lactococcus lactis*, Amp^R	this lab
pETaDat	pET21a-*Dat*, pET21a carries a d-amino acid transaminase (*Dat*) gene from *Bacillus subtilis*, Amp^R	this lab
pETaVfl	pET21a-*Vfl*, pET21a carries an alpha-ketoacid decarboxylase (*KdcA*) gene from *Lactococcus lactis*, Amp^R	this lab
pWD01	pZA22-*leuA-leuB-leuC-leuD*, pZA22 carries a 2-isopropylmalate synthase (*leuA*) gene, a 3-isopropylmalate dehydrogenase (*leuB*) gene, a 3-isopropylmalate dehydratase large subunit (*leuC*) gene, and a 3-isopropylmalate dehydratase small subunit (*leuD*) gene from *Escherichia coli*, Kan^R	this lab
pWD02	pZA22-*leuA**-*leuB-leuC-leuD*, pZA22 carries a 2-isopropylmalate synthase mutant (H97L/S139G/G462D) gene, a 3-isopropylmalate dehydrogenase (*leuB*) gene, a 3-isopropylmalate dehydratase large subunit (*leuC*) gene, and a 3-isopropylmalate dehydratase small subunit (*leuD*) gene from *Escherichia coli*, Kan^R	this lab
pETaRVK	pET21a-*Raip-Vfl-kivD*, pET21a carries a l-lysine α-oxidase (*Raip*) gene from *Scomber japonicas*, a pyruvate transaminase (*Vfl*) gene from *Vibrio fluvialis,* and a α-ketoacid decarboxylase (*kivD*) gene from *Lactococcus lactis*, Amp^R	this study
pETaRKD	pET21a-*Raip-KdcA-Dat*, pET21a carries a l-lysine α-oxidase (*Raip*) gene from *Scomber japonicas*, an alpha-ketoacid decarboxylase (*KdcA*) gene from *Lactococcus lactis,* and a d-amino acid transaminase (*Dat*) gene from *Bacillus subtilis*, Amp^R	this study
pETaRKP	pET21a-*Raip-KivD-pATA*, pET21a carries a L-lysine α-oxidase (*Raip*) gene from *Vibrio fluvialis* and a α-ketoacid decarboxylase (*KivD*) gene from *Lactococcus lactis* and a putrescine transaminase (*pATA*) gene from *Escherichia coli*, Amp^R	this study
pETaRDL	pET21a-*Raip-Dat-lysA*, pET21a carries a l-lysine α-oxidase (*Raip*) gene from *Vibrio fluvialis* and a d-amino acid transaminase (*Dat*) gene from *Bacillus subtilis* and a diaminopimelate decarboxylase (*lysA*) gene from S. clavuligerus, Amp^R	this study

are available in the GenBank database with accession numbers of MG423617, AIS03677.1, NC_000964.3, AAS49166.1, and HQ418483.1, respectively. The *Raip*, *KivD*, and *Vfl* genes were constructed in a single operon with the transcriptional order of *Raip-Vfl-KivD* first; subsequently, the modified pET21a-*Raip-Vfl-KivD* plasmid was created. This construct was also designated as pETRVK. *KivD* was replaced by $KivD^{\#}$ (*KivD**, *KivD* with F381L/V461A mutations) to form the engineered pET21a-*Raip-Vfl-*$KivD^{\#}$, also named as $pETRVK^{\#}$. The genes for *Raip*, *Dat*, and *KdcA* were assembled into a single transcriptional unit with the sequence *Raip-KdcA-Dat*. Consequently, the engineered plasmid pET21a-*Raip-KdcA-Dat* was generated, which is also referred to as pETRKD.

Protein Expression and Purification. A volume of 1 mL from the precultures of the genetically modified *E. coli*, which had been incubated overnight, was introduced into 50 mL of new Luria−Bertani (LB) medium within a 250 mL shaking flask. The flasks were supplemented with ampicillin and kanamycin, and the cultures were grown at a temperature of 37 °C with a shaking speed of 200 rpm. When the OD_{600} reached a value of 0.6, the production of recombinant proteins was initiated by adding IPTG to a final concentration of 0.6 mM in the bacterial cultures. After induction, the cultures were further incubated at a reduced temperature of 30 °C for an extended period, typically overnight. Cells were then harvested by centrifugation, washed with fresh potassium phosphate buffer (KPB, 50 mM, pH 8.0), and resuspended in 50 mL of KPB to OD_{600} = 3. Subsequently, cells were resuspended and their membranes were disrupted by sonication in a buffer solution comprising 250 mM sodium chloride (NaCl), 2 mM dithiothreitol, 5 mM imidazole, and 50 mM Tris adjusted to a pH of 9.0. A stepwise increase in imidazole concentration, up to 250 mM, was utilized to purify the enzymes from the cell lysates via Ni-NTA affinity column chromatography. The presence of the expressed enzymes was confirmed by running a 10% SDS-PAGE and visualizing the bands with Coomassie Brilliant Blue staining. Fermentation conditions for HMD production in shake flasks. A single colony from the target strain was grown in a LB medium, supplemented with the necessary antibiotics, for an extended period (12−16 h) to form an overnight culture. This culture was then utilized as the starting inoculum at an OD_{600} equal to 0.5. Then, 2% (v/v) cultures were cultured in the 50 mL medium containing 15 g/L glucose, 10 g/L tryptone, 5 g/L yeast extract, 0.1 g/L $FeCl_3$, 2.1 g/L citric acid·H_2O, 2.5 g/L $(NH_4)2SO_4$, 0.5 g/L K_2PO_4·$3H_2O$, 3 g/L KH_2PO_4, and 1.0 mM $MgSO_4$ with appropriate antibiotics. After inoculation, flasks were incubated at 37 °C and 200 rpm until OD_{600} reached 0.4−0.8, at which point IPTG (0.5 mM), L-lysine (5.0 g/L), NAD^+ (1.0 mM), Gln (1 g/L), ThDP (0.5 mM), Ala (1 g/L), and Acyl-CoA (1 mM) were added to induce enzyme expression at 30 °C. Unless specified otherwise, the flasks continued to be incubated under identical conditions for a duration of 48 h postinduction.

Analysis. As Fedorchuk reported,[4] liquid chromatography−mass spectrometry (LC−MS) analysis of reaction products (PMD and HMD) was performed using a Dionex Ultimate

https://doi.org/10.1021/acsomega.4c06289
ACS Omega 2024, 9, 40970−40979

3000 UHPLC system and a QExactive mass spectrometer equipped with a HESI-II probe (all from Thermo Scientific) and controlled by Thermo XCalibur 4.1 software. LC separation was conducted on a Hypersil Gold C18 column (50 mm × 2.1 mm, 1.9 μm particle size, Thermo Scientific) equipped with a guard column, column temperature 40 °C. Solvent A was 0.1% formic acid (in water), solvent B was 0.1% formic acid in methanol (flow rate 1 mL/min). Autosampler temperature was maintained at 8 °C, and injection volume was 1 μL. The gradient was 0−1.5 min: 100% A; 1.5−7.0 min: 0% A, 100% B; 10−11 min: 100% A, 0% B; and 11.0−15.0 min: 100% A. Data collection was done in positive ionization mode with a scan range m/z 90−200, resolution 140 000 at 1 Hz, AGC target of 3e6 ions and a maximum injection time of 250 ms. Standard solutions of HMD (m/z 117.15) and PMD (m/z 103.15) were used for validation of retention time and m/z. The concentration of L-lysine was detected as reported in our previous work.

Enzyme Assay. *KivD*. The kinetic parameters kcat and Km of *KivD* and its variants were determined for 2-ketoheptanoic acid decarboxylation at 30 °C using a coupled assay with excess *ADH* in yeast. The reaction's progress was monitored by reduced nicotinamide adenine dinucleotide (NADH) consumption at 340 nm over 30 min in a 96-well plate with a microplate spectrophotometer. The assay mixture contained NADH, dithiothreitol, TPP, $MgSO_4$, and variable *ADH* concentrations in K_3PO_4 buffer, pH 7.4. The reaction was initiated with purified *KivD*, and steady-state kinetics were established by using varying enzyme concentrations. The initial velocity measurements were applied to the Michaelis−Menten kinetic model to determine the kcat and Km. The standard deviations associated with these values represent the errors in the fitting process.

KdcA. The decarboxylation of 2-keto acids was measured at 30 °C using a modified coupled enzymatic assay. The assay mixture contained 0.2 mM NADH, 0.5 units/mL horse liver alcohol dehydrogenase, and the 2-keto acid in assay buffer (50 mM K_3PO_4 buffer, pH 6.0, 1 mM $MgSO_4$, and 0.5 mM ThDP) in a total volume of 1 mL. The reaction was initiated by adding 0.5−100 ng of enzyme diluted in storage buffer, and the consumption of NADH was monitored at 340 nm with a Cary 50 Bio spectrophotometer (Varian). One unit is defined as the amount of enzyme that catalyzes the decarboxylation of 1 μmol 2-keto acid per minute at 30 °C under standard conditions.

Dat. Under the condition of 37 °C, the activity of D-amino acid transaminase was determined by a coupled enzyme assay system. The transaminase converted D-alanine and α-ketoglutarate acid into D-glutamate and pyruvate. The lactate dehydrogenase converted the pyruvic acid into lactic acid. The results of the latter reaction were the oxidation of NADH to NAD^+, which can be followed by spectrophotometry at 340 nm. The initial blank was Tris−HCl (PH 8.5, 100 mM), and the reagents were added sequentially. The kinetic evaluation commenced with the introduction of NADH at a final concentration of 300 mM. After a 3 min interval, either undiluted or diluted (by factors of 10 or 100) crude sonicate was introduced in a volume of 10 μL. Subsequently, at the 6 min mark, 10 units of lactate dehydrogenase were added. α-Ketoglutarate, at a final concentration of 25 mM, was incorporated at the 9 min point. The sequence concluded at the 12 min mark with the addition of D-alanine, also at a final concentration of 25 mM, to initiate the enzymatic reaction. Throughout this process, D-glutamic acid underwent racemization to its L-enantiomer, which was subsequently transformed to α-ketoglutarate by the action of L-glutamate dehydrogenase. Nicotinamide adenine dinucleotide phosphate was reduced to reduced nicotinamide adenine dinucleotide phosphate by this reaction and could be tracked through the spectrophotometer at 340 nm.

Vfl. The *E. coli* derivatives were grown in LB, where 100 μg/mL ampicillin was added until an optical density at 600 nm of 0.6−0.8, induced with 0.6 mM IPTG, and harvested in the exponential phase at OD_{600} = 3.5. The cells were washed with 100 mM K_3PO_4 buffer with pH 7.4. The reaction conditions were as follows: 100 mM K_3PO_4 buffer (PH 7.4), 50 mM (*S*)-α-MBA, and 10 mM pyruvate. The transamination was initiated upon the addition of a crude extract, and samples were taken continuously. The reaction was stopped with 75 μL of 16% perchloroacetic acid. The samples where neutralized by the addition of 40 μL of buffer containing 20 mM Tris−HCl pH 8 and 23 mM K_2CO_3. The formation of L-alanine was determined by HPLC, and one enzyme unit was calculated to be the amount of enzyme to catalyze the formation of 1 μmol product in 1 min.

Calculation of Gibbs Free Energy. The thermodynamic feasibility of these theoretical cycles was first evaluated by calculating their Gibbs free energy profile ($\Delta rG'$) under biologically relevant conditions. Gibbs free energy values for all reactions were calculated by eQuilibrator (https://equilibrator.weizmann.ac.il/) or taken from literature, as indicated in Table S1.

ATP Analysis. The BacTiter-GloMicrobial Cell Viability Assay (Promega Corporation) and a high-sensitivity photon-counting luminometer (SpectraMax M5; Molecular Devices) were used for measuring the ATP luminescence (relative light unit, RLU). The protocol recommends a volume of reagent equal to the volume of cell culture present in each well and ensures that the temperature of the sample and ATP reagent are constant. The reagent volume was set to 50 mL and the sample volumes were 50, 100, and 150 mL, respectively. The maximum luminescence of the 150 mL sample was selected to investigate the influence of incubation temperatures (25−42 °C).

Statistical Analysis. The statistical significance of the data collected in this research was determined using the two-tailed *t*-test approach. A p value of less than 0.05 was considered to indicate a statistically significant result.

■ ASSOCIATED CONTENT

Data Availability Statement

All data included in this study are available upon request by contact with the corresponding author.

Supporting Information

The Supporting Information is available free of charge at https://pubs.acs.org/doi/10.1021/acsomega.4c06289.

SDS-PAGE of key enzymes, Gibbs free energies used to calculate Gibbs free energy profiles, main oligonucleotide primers used in this study, and information of enzymes used in the enzymatic platform (PDF)

■ AUTHOR INFORMATION

Corresponding Author

Dan Wang − *Department of Chemical Engineering, School of Chemistry and Chemical Engineering, Chongqing University, Chongqing 401331, P. R. China;* orcid.org/0000-0002-

https://doi.org/10.1021/acsomega.4c06289
ACS Omega 2024, 9, 40970−40979

8529-1665; Phone: 86-23-65678926; Email: dwang@cqu.edu.cn

Authors

Kaixing Xiao − *Department of Chemical Engineering, School of Chemistry and Chemical Engineering, Chongqing University, Chongqing 401331, P. R. China*

Xuemei Liu − *Department of Chemical Engineering, School of Chemistry and Chemical Engineering, Chongqing University, Chongqing 401331, P. R. China*

Yaqi Kang − *Department of Chemical Engineering, School of Chemistry and Chemical Engineering, Chongqing University, Chongqing 401331, P. R. China*

Ruoshi Luo − *Department of Chemical Engineering, School of Chemistry and Chemical Engineering, Chongqing University, Chongqing 401331, P. R. China*

Lin Hu − *Department of Chemical Engineering, School of Chemistry and Chemical Engineering, Chongqing University, Chongqing 401331, P. R. China*

Zhiyao Peng − *Department of Chemical Engineering, School of Chemistry and Chemical Engineering, Chongqing University, Chongqing 401331, P. R. China*

Complete contact information is available at: https://pubs.acs.org/10.1021/acsomega.4c06289

Author Contributions

K.X. and D.W. conceived and designed the experiments; K.X., Y.K., X.L., and L.H. performed the experiments. D.W. and R.L. helped guide the pathway analyzing and gene editing; K.X. and D.W. analyzed the experimental data; and K.X., Y.K., and Z.P. wrote the manuscript. All authors approved the final manuscript.

Notes

The authors declare no competing financial interest.

■ ACKNOWLEDGMENTS

This work was supported by the National Key Research and Development Program of China (2022YFC2105700); the National Natural Science Foundation of China (22378032); Chongqing Outstanding Youth Fund (cstc2021jcyj-jqX0013), the Human Resources and Social Security Bureau of Chongqing (cx2023036).

■ ABBREVIATIONS

HMD	1,6-hexamethylenediamine;
DAP	1,5-diaminopentane
DAHP	1,7-diaminoheptane
Raip	L-lysine α oxidase
LeuA	α-Isopropylmalate synthase
*LeuA**	LeuA mutants
LeuA$^{\#}$	LeuA with H97L/S139G/G462D mutations
LeuB	3-isopropylmalate dehydrogenase
LeuC	3-isopropylmalate dehydratase
LeuD	3-isopropylmalate dehydratase
KivD	α-ketoacid decarboxylase
DAT	D-alanine aminotransferase
KdcA	alpha-ketoacid decarboxylase
6ACA	6-aminocaproate
2K6AC	2-keto-6-aminocaproate
7A2OPA	7-amino-2-oxoheptanoic acid
NNSCAA	non-natural straight chain amino acid

■ REFERENCES

(1) The first nylon plant. *Am. Chem. Soc.* **1995**, 1−8.
(2) Nopparut, A.; Amornsakchai, T. Influence of pineapple leaf fiber and it's surface treatment on molecular orientation in, and mechanical properties of, injection molded nylon composites. *Polym. Test.* **2016**, *52*, 141−149.
(3) Zhang, C.; Cao, M.; Jiang, S.; Huang, X.; Mai, K.; Yan, K. Quick analysis of composition of semi-aromatic copolyamide via 13C NMR study. *Int. J. Polym. Anal. Charact.* **2019**, *24* (1), 40−53.
(4) Fedorchuk, T. P.; Khusnutdinova, A. N.; Evdokimova, E.; Flick, R.; Di Leo, R.; Stogios, P.; Savchenko, A.; Yakunin, A. F. One-pot biocatalytic transformation of adipic acid to 6-aminocaproic acid and 1, 6-hexamethylenediamine using carboxylic acid reductases and transaminases. *J. Am. Chem. Soc.* **2020**, *142* (2), 1038−1048.
(5) Turk, S. C.; Kloosterman, W. P.; Ninaber, D. K.; Kolen, K. P.; Knutova, J.; Suir, E.; Schurmann, M.; Raemakers-Franken, P. C.; Muller, M.; de Wildeman, S. M.; et al. Metabolic engineering toward sustainable production of nylon-6. *ACS Synth. Biol.* **2016**, *5* (1), 65−73.
(6) Cheng, J.; Hu, G.; Xu, Y.; Torrens-Spence, M. P.; Zhou, X.; Wang, D.; Weng, J.-K.; Wang, Q. Production of nonnatural straight-chain amino acid 6-aminocaproate via an artificial iterative carbon-chain-extension cycle. *Metab. Eng.* **2019**, *55*, 23−32.
(7) Deng, Y.; Mao, Y. Production of adipic acid by the native-occurring pathway in Thermobifida fusca B6. *J. Appl. Microbiol.* **2015**, *119* (4), 1057−1063.
(8) Zhang, Z.; Fang, L.; Wang, F.; Deng, Y.; Jiang, Z.; Li, A. Transforming Inert Cycloalkanes into α, ω-Diamines by Designed Enzymatic Cascade Catalysis. *Angew. Chem., Int. Ed.* **2023**, *62* (16), No. e202215935.
(9) Li, J. M.; Shi, K.; Li, A. T.; Zhang, Z. J.; Yu, H. L.; Xu, J. H. Development of a Thermodynamically Favorable Multi-enzyme Cascade Reaction for Efficient Sustainable Production of ω-Amino Fatty Acids and α, ω-Diamines. *ChemSusChem* **2024**, *17* (6), No. e202301477.
(10) Wang, L.; Li, G.; Li, A.; Deng, Y. Directed synthesis of biobased 1, 6-diaminohexane from adipic acid by rational regulation of a functional enzyme cascade in Escherichia coli. *ACS Sustainable Chem. Eng.* **2023**, *11* (15), 6011−6020.
(11) Mormul, J.; Breitenfeld, J.; Trapp, O.; Paciello, R.; Schaub, T.; Hofmann, P. Synthesis of adipic acid, 1, 6-hexanediamine, and 1, 6-hexanediol via double-n-selective hydroformylation of 1, 3-butadiene. *ACS Catal.* **2016**, *6* (5), 2802−2810.
(12) Wang, L.; Zhang, C.; Zhang, J.; Rao, Z.; Xu, X.; Mao, Z.; Chen, X. Epsilon-poly-L-lysine: recent advances in biomanufacturing and applications. *Front. Bioeng. Biotechnol.* **2021**, *9*, 748976.
(13) Wang, J.; Gao, C.; Chen, X.; Liu, L. Expanding the lysine industry: Biotechnological production of L-lysine and its derivatives. *Adv. Appl. Microbiol.* **2021**, *115*, 1−33.
(14) Torrens-Spence, M. P.; Weng, J.-K. *Production of nonnatural straight-chain amino acid 6-aminocaproate via an artificial iterative carbon-chain-extension cycle*; Elsevier BV, 2019; .
(15) Xu, J.-Z.; Wu, Z.-H.; Gao, S.-J.; Zhang, W. Rational modification of tricarboxylic acid cycle for improving L-lysine production in Corynebacterium glutamicum. *Microb. Cell Factories* **2018**, *17*, 105.
(16) Paulikat, M.; Wechsler, C.; Tittmann, K.; Mata, R. A. Theoretical studies of the electronic absorption spectra of thiamin diphosphate in pyruvate decarboxylase. *Biochemistry* **2017**, *56* (13), 1854−1864.
(17) Lietzan, A. D.; Maurice, M. S. A substrate-induced biotin binding pocket in the carboxyltransferase domain of pyruvate carboxylase. *J. Biol. Chem.* **2013**, *288* (27), 19915−19925.
(18) Chen, G. S.; Siao, S. W.; Shen, C. R. Saturated mutagenesis of ketoisovalerate decarboxylase V461 enabled specific synthesis of 1-pentanol via the ketoacid elongation cycle. *Sci. Rep.* **2017**, *7* (1), 11284.
(19) Gocke, D.; Nguyen, C. L.; Pohl, M.; Stillger, T.; Walter, L.; Müller, M. Branched-Chain Keto Acid Decarboxylase from

Lactococcus lactis (KdcA), a Valuable Thiamine Diphosphate-Dependent Enzyme for Asymmetric C□ C Bond Formation. *Adv. Synth. Catal.* **2007**, *349* (8−9), 1425−1435.
(20) Milne, N.; Van Maris, A.; Pronk, J.; Daran, J. Comparative assessment of native and heterologous 2-oxo acid decarboxylases for application in isobutanol production by Saccharomyces cerevisiae. *Biotechnol. Biofuels* **2015**, *8*, 204.
(21) Wang, M.; Maeda, H. A. Aromatic amino acid aminotransferases in plants. *Phytochemistry Rev.* **2018**, *17*, 131−159.
(22) Dimou, A.; Tsimihodimos, V.; Bairaktari, E. The critical role of the branched chain amino acids (BCAAs) catabolism-regulating enzymes, branched-chain aminotransferase (BCAT) and branched-chain α-keto acid dehydrogenase (BCKD), in human pathophysiology. *Int. J. Mol. Sci.* **2022**, *23* (7), 4022.
(23) Li, T.; Cui, X.; Cui, Y.; Sun, J.; Chen, Y.; Zhu, T.; Li, C.; Li, R.; Wu, B. Exploration of transaminase diversity for the oxidative conversion of natural amino acids into 2-ketoacids and high-value chemicals. *ACS Catal.* **2020**, *10* (14), 7950−7957.
(24) Darby, J. F.; Gilio, A. K.; Piniello, B.; Roth, C.; Blagova, E.; Hubbard, R. E.; Rovira, C.; Davies, G. J.; Wu, L. Substrate engagement and catalytic mechanisms of N-acetylglucosaminyltransferase V. *ACS Catal.* **2020**, *10* (15), 8590−8596.
(25) Jeong, S. Y.; Jin, H.; Chang, J. H. Crystal structure of L-aspartate aminotransferase from Schizosaccharomyces pombe. *PLoS One* **2019**, *14* (8), No. e0221975.
(26) Bujacz, A.; Rum, J.; Rutkiewicz, M.; Pietrzyk-Brzezinska, A. J.; Bujacz, G. Structural evidence of active site adaptability towards different sized substrates of aromatic amino acid aminotransferase from Psychrobacter sp. B6. *Materials* **2021**, *14* (12), 3351.
(27) Shin, J. H.; Park, S. H.; Oh, Y. H.; Choi, J. W.; Lee, M. H.; Cho, J. S.; Jeong, K. J.; Joo, J. C.; Yu, J.; Park, S. J.; et al. Metabolic engineering of Corynebacterium glutamicum for enhanced production of 5-aminovaleric acid. *Microb. Cell Factories* **2016**, *15*, 174.
(28) Shimizu, K.; Matsuoka, Y. Feedback regulation and coordination of the main metabolism for bacterial growth and metabolic engineering for amino acid fermentation. *Biotechnol. Adv.* **2022**, *55*, 107887.
(29) Sukonina, V.; Ma, H.; Zhang, W.; Bartesaghi, S.; Subhash, S.; Heglind, M.; Foyn, H.; Betz, M. J.; Nilsson, D.; Lidell, M. E.; et al. FOXK1 and FOXK2 regulate aerobic glycolysis. *Nature* **2019**, *566* (7743), 279−283.
(30) Li, J.; Mara, P.; Schubotz, F.; Sylvan, J. B.; Burgaud, G.; Klein, F.; Beaudoin, D.; Wee, S. Y.; Dick, H. J.; Lott, S.; et al. Recycling and metabolic flexibility dictate life in the lower oceanic crust. *Nature* **2020**, *579* (7798), 250−255.
(31) Schönknecht, G.; Chen, W.-H.; Ternes, C. M.; Barbier, G. G.; Shrestha, R. P.; Stanke, M.; Bräutigam, A.; Baker, B. J.; Banfield, J. F.; Garavito, R. M.; et al. Gene transfer from bacteria and archaea facilitated evolution of an extremophilic eukaryote. *Science* **2013**, *339* (6124), 1207−1210.
(32) Xue, Y.; Zhao, Y.; Ji, X.; Yao, J.; Busk, P. K.; Lange, L.; Huang, Y.; Zhang, S. Advances in bio-nylon 5X: discovery of new lysine decarboxylases for the high-level production of cadaverine. *Green Chem.* **2020**, *22* (24), 8656−8668.

https://doi.org/10.1021/acsomega.4c06289
ACS Omega 2024, 9, 40970−40979